Astron. Astrophys. 209, 165–172 (1989)

ASTRONOMY
AND
ASTROPHYSICS

IRAS Low Resolution Spectrograph spectral class and M and S Miras

M.S. Vardya

Tata Institute of Fundamental Research, Homi Bhabha Road, Bombay 400005, India

Received February 16, accepted July 18, 1988

Summary. A large sample of 177 M and S Miras, as revealed by their IRAS LRS spectral class, have been examined to determine the dependence of silicate emission on the visual light curve aysmmetry factor, f. It is confirmed that 9.7 μm silicate emission feature not only in M but in S Miras also occurs only when $f \leqq 0.45$. However, not all stars with $f \leqq 0.45$ show the silicate emission; this non-detection reveals dependence on other parameters like the mean visual light amplitude. Though strong emission feature in M Miras may occur for any value of f, very weak features are absent for small values of f and the strongest features tend to appear for larger values of f. Infrared excess tends to increase with the strength of the silicate emission as well as with decrease in the value of f. Probability of detection of silicate emission is very high for visual light curve classes (Ludendorff) α_1, α_2 and α_3, decreases for α_4 and γ_1, and is negligible for β class.

Key words: stars: long period variables – stars: circumstellar matter – stars: visual light curve – stars: far infrared spectroscopy

1. Introduction

A large number of M spectral type Mira variables show strong silicate emission features at 9.7 and 20 μm among the Low Resolution Spectrograph (LRS) spectra obtained with the Infrared Astronomical Satellite (IRAS). Vardya et al. (1986) found that the 9.7 μm emission seems to occur only in the spectra of those Miras with visual light asymmetry factor $f \leqq 0.45$; here f is defined as the ratio of the number of days between minimum light and the next following maximum to the period. The main study was based on the visual inspection of the LRS spectra of 19 Miras, supplemented by an additional 27 Miras to check the conclusion. This has been extended by Onaka and de Jong (1987) by analysing the LRS spectra of 109 M Miras. Here, we have examined this earlier work of Vardya et al. (1988) but depart from it as well as the work of Onaka and de Jong (1987) by:

(i) using IRAS LRS spectral class, rather than spectra itself, as given in the Point Source Catalogue, making the analysis somewhat quantitative;

(ii) using all Mira variable stars, not only of M but of S spectral type also, which may possibly exhibit oxygen rich circumstellar chemistry, as determined by the IRAS LRS spectral classes 1n, 2n, 3n, 5n, 6n and 7n (Beichman et al., 1985), and having known value of f; and

(iii) using Ludendorff's visual light curve class also, besides the asymmetry factor f.

This sample thus comprises of 177 stars with 164 M and 13 S Miras.

2. Sample of stars

Among the objects with LRS spectral code, 1n, 2n, 3n, 5n, 6n and 7n, we have considered all the M and S Miras for which visual light asymmetry factor f is known (Kholopov, 1985). This gives a sample of 164 M Miras and 13 S Miras. We have not considered LRS class 0n, as they denote either very noisy spectra or strange band shape.

Table 1a gives the variable name of the star, period in days, visual light asymmetry factor f, spectral class, IRAS LRS spectral class, mean visual light amplitude (Kukarkin et al., 1969), $\log S_{12}/S_{25}$, and visual light curve class for M spectral type Mira variables; here S_{12} and S_{25} are the flux densities at 12 and 25 μm, respectively. Table 1b gives similar data for S Miras along with the NSS number from the S star catalogue of Stephenson (1984). The last column gives remarks if any. Flux densities of high quality (class 3) only have been included in the tables.

3. Results

Table 1 shows that the stars in our sample are equally divided among LRS classes 1n and 2n, with one star each in 3n and 5n, two in 6n class, and none in 7n. Except for five stars, all M Miras with LRS classes 2n and 6n have $f \leqq 0.45$; among the five exceptions (V845 Aql, X Ara, Z Sgr, IK Tau and S UMi), V845 Aql has the strongest silicate signature with LRS class 69 but its f value is uncertain, and the flux density low. The f value for IK Tau is from recent data and may not be a good average value. The remaining three stars have LRS class 21 or 22 i.e. weak silicate features. The spectra of X Ara and Z Sgr are rather noisy (Olnon and Raimond, 1986), their flux density low, and the LRS class may or may not be a true indicator of silicate emission feature; the value of f for X Ara may be based on limited data. The very low values of $\log S_{12}/S_{25}$ for V845 Aql, X Ara, and IK Tau are more appropriate for $f \leqq 0.43$. In the fifth star, S UMi, the silicate feature is very weak, and the spectrum is an average of two spectra only. Note that the LRS classes 21 and 22 may reflect noise in some of the stars. Thus we see that this large data essentially confirms the result obtained by Vardya et al. (1986) that 9.7 μm silicate emission in M Miras is present only when $f \leqq 0.45$. In rare cases, silicate feature may be present for $f > 0.45$, but a good case needs to be found for confirmation. Only one Mira (R Cha) has a LRS class 3n, i.e., 31, indicating 9.7 μm silicate absorption. This being a

very weak feature, we checked the LRS spectrum (Olnon and Raimond, 1986) and found that it can be due to noise. However, not all M Miras with $f \leqq 0.45$ show 9.7 μm silicate emission; in fact, about one fifth of these Miras have LRS class 1n. This non-detection can be due to (a) noisy spectra, (b) self absorption of the silicate feature, (c) blowing away or dissipation of the circumstellar shell, the seat of the emission feature or/and (d) dependence of this feature on parameters besides f. Examining the last possibility, we find that the maximum number of non-detection ($\sim 60\%$) is in the region $0.43 < f \leqq 0.45$, which is a kind of transition region, and for $f < 0.36$, all stars appear to have silicate emission feature. Further, non-detection of stars is as high as $\sim 45\%$ for mean visual light amplitude, $\langle \Delta M_V \rangle \leqq 5^m.0$ but decreases to $\sim 18\%$ for $\langle \Delta M_V \rangle > 5^m.0$ (Fig. 1). Remember that for $f < 0.36$, silicate emission has been observed even from a star, DH Cyg, with $\langle \Delta M_V \rangle = 2^m.3$.

Whether RT Oph is a M spectral type star or a C star, is not certain; its spectral class, as given in Kholopov (1985) is M7e(C), but it is not in the Carbon Star Catalogue (Stephenson, 1973). Further, the f value of 0.19 for CH Pup, of 0.25 for AA Sct and of 0.5 for IK Tau may be wrong. Ignoring these four stars, if we plot the LRS spectral class (2 or 6)n vs f for $f \leqq 0.45$, we find (Fig. 2) that for LRS class (2 or 6)n, $n \geqq 4$ covers all stars with $f < 0.37$, but only two fifth of the stars with $0.37 < f < 0.45$, and for LRS class (2 or 6)n, $n \geqq 3$ covers all stars with $f < 0.39$ but only two third stars with $0.39 < f < 0.45$. Further, the weakest (21, 22) and the strongest (29, 69) emission features have a tendency to appear for larger values of f. This implies that strong 9.7 μm silicate emission can be present for any $f \leqq 0.45$, but lower f values appears to have only strong silicate emission feature. However, all six stars with LRS spectral class (2 or 6) 9 have $f \geqq 0.38$.

Figure 3 gives a plot of $\log S_{12}/S_{25}$ vs. f. Here S_{12} and S_{25} are the observed fluxes at 12 and 25 μm taken from the IRAS Point Source Catalogue. Plotted are mean values of $\log S_{12}/S_{25}$ of stars with given f. The mean of 5 or more points is shown by a circle, and of 4 stars by a square. The extent of variation at a given f

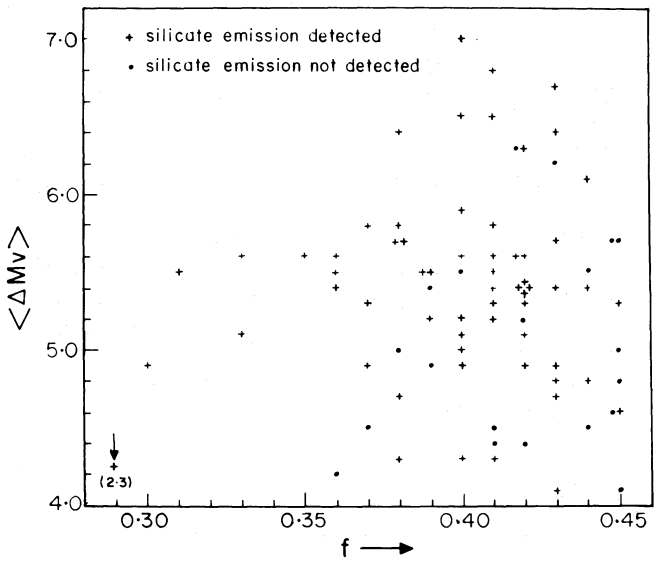

Fig. 1. The mean visual light amplitude vs. f for M Miras for stars with and without silicate emission features are marked plus (+) and dots (·)

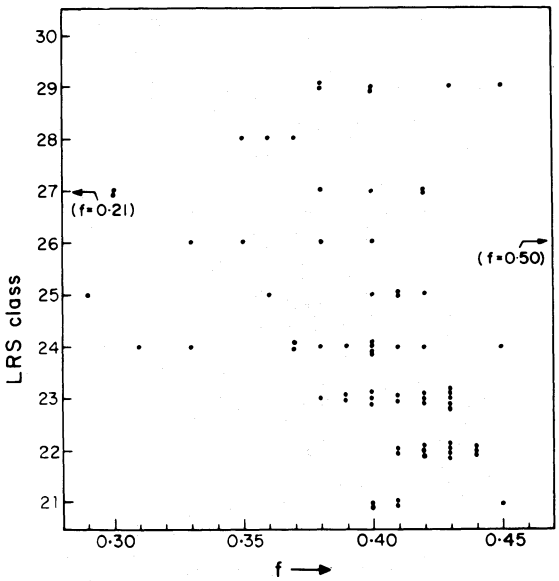

Fig. 2. Plot of IRAS LRS spectral class vs. f for M Miras. Note that LRS class 29 includes LRS class 69 stars

Table 1a. Data for M spectral type Miras

Star name	Period (day)	$f \times 10^2$	Spectral type	LRS class	$\langle \Delta M_v \rangle$	log S_{12}/S_{25}	l.c.c. (55)	Remarks
U And	347	41	M6e	15	4.4	0.349	α_3	
SV	316	38	M5e-7e	16	5.0	0.411	α_2	7
TU	317	48	M5e	15	4.0	0.430	—	1
W Aqr	381	42	M6e-8e	22	5.3	0.403	α_3	
Y	382	43	M6.5e-9	23	5.4	0.367	α_2	
R Aql	284	42	M5e-9e	23	5.4	0.216	α_4	137
RR	395	30	M6e-9	27	4.9	0.343	α_3	3
RS	410	48	M5e-8	14	5.5	0.432	α_2	
RT	327	42	M6e-8e(S)	24	5.6	0.324	α_3	3
SY	356	37	M5e-7e	28	4.9	0.300	α_3	56
V845	229	50:	—	69	—	0.168	—	

Table 1a (continued)

Star name	Period (day)	$f \times 10^2$	Spectral type	LRS class	$\langle \Delta M_v \rangle$	log S_{12}/S_{25}	l.c.c. (55)	Remarks
X Ara	176	51	M5e-7eII-III	22	—	0.284	—	
U Ari	371	40	M4e-9.5e	21	6.5	0.431	α_2	4
R Aur	458	51	M6.5e-9.5e	15	5.6	0.399	γ_1	12
U	408	39	M7e-9e	23	5.5	0.324	α_2	5
RU	466	40	M7e-9e	25	4.9	0.279	α_1	6
SZ	454	46	M8e	15		0.397	—	
R Boo	223	46	M3e-8e	14	5.1	0.361	β_1	
RT	274	49	M6.5e-8e	15	4.5	0.374	—	
R Cae	391	41	M6e	23	5.2	0.371	α_2	
V Cam	522	31	M7e	24	5.5	0.285	α_2	45
R Cnc	362	47	M6e-9e	15	4.4	0.430	α_4	4
W	393	40	M6.5e-9e	23	5.9	0.294	α_3	
R CVn	329	46	M5.5e-9e	15	4.2	0.404	β_2	1
S CMi	333	49	M6e-8e	15	5.1	0.402	β_1	
V Cap	276	42	M5e-8.2	27	—	0.169	α_2	
RU	347	36	M9e	28	5.4	0.189	α_3	2
R Car	309	48	M4e-8e	15	5.0	0.445	β_1	245
S	149	51	K5e-M6e	17	2.8	0.509	β_3	
Z	384	37	M6e	15	4.5	0.372	α_3:	
RV	366	39	M6e	14	4.9	0.356	γ_1	
RW	319	47	M4e-7e	15	5.7	0.388	α_3	
RZ	273	42	M4e-8e	25	5.4	0.385	—	
R Cas	430	40	M6e-10e	24	5.6	0.383	γ_1	3467
T	445	56	M6e-9.0e	15	4.0	0.381	γ_1	47
V	229	48	M5e-8.5e	16	4.3	0.436	β_2	
Y	413	43	M6e-8.5e	22	4.7	0.319	α_2	3
RV	332	38	M4.5e-9.5e	23	5.8	0.318	γ_1	
MP	338	50	M8	51	—	−0.805		7
W Cen	202	47	M3e-8(III)e	15	4.7	0.381	β_1	
X	315	41	M5e-6.5e	23	5.4	0.416	α_4	
RT	255	47	M6II:e	15	3.7	0.418	β_3	1
RX	328	38	M5e	15	—	0.318	α_2	
TW	269	43	M4e-8II:	22	—	0.440	—	
T Cep	388	54	M5.5e-8.8e	15	4.3	0.452	γ_1	14
X	535	42	M4.5e-7e	23	6.3	0.311	α_2	6?
Y	333	40	M5e-8.2e	14	5.5	0.410	α_3	
RR	384	41	M5e-8.8e	14	4.5	0.314	α_2	
R Cet	166	43	M4e-9	29	4.9	0.134	α_4	
R Cha	335	41	M4e-7e	31	5.1	0.436	α_4	
R Col	328	39	M3e-7	15	5.4	0.301	α_1	
S	326	46	M6e-8	14	4.5	0.354	α_3	
T	226	50	M3e-6e	16	4.4	0.427	β_2	4
R Com	363	38	M5e-8ep	24	5.7	0.277	α_2	6
S CrB	360	33	M6e-8e	24	5.6	0.204	α_2	3
Z Cyg	264	45	M5e-9e	69	4.6	0.083	α_2	567
SX	411	41	M7e	21	5.3	0.340	α_2	
TW	341	48	M6.5-10ep	16	4.5	0.408	α_4	
UX	565	40	M4e-6.5e	29	—	0.228:	α_1	13
BG	288	50	M7e-8e	15	—	0.423	—	1
DH	528	29	M6	25	2.3	0.185	—	6?
KZ	406	45	M8e	21	—	0.352	—	
R Del	285	45	M5e-6e	15	5.0	0.417	α_4	
S	278	52	M5e-8	16	3.2	0.413	β_2?	27
V	534	42	M4e-6e	22	5.4	0.170	α_1	

Table 1a (continued)

Star name	Period (day)	$f \times 10^2$	Spectral type	LRS class	$\langle \Delta M_v \rangle$	log S_{12}/S_{25}	l.c.c. (55)	Remarks
Y Del	468	43	M8e	23	4.1	0.222	α_1	
R Dra	246	45	M5e-9eIII	16	4.8	0.390	α_4	
U	316	47	M6e-8	15	4.3	0.406	β_1	1
Y	326	45	M5e	24	5.3	0.397	α_2	
T Eri	252	45	M3e-5e	16	4.8	0.452	α_4	
W	377	40	M7e-9	24	5.2	0.362	α_3	3
RT	371	46	M7e	15	—	0.407	—	
S Gem	293	42	M4e-8e	17	5.2	0.399	α_3	2
X	264	49	M5e-8e(Tc)	17	5.0	0.412	β_2	
R Gru	332	42	M5e-7II-IIIe	15	6.3	0.374	α_4	
S	402	43	M5e-8IIe	22	6.7	0.349	γ_1	
U Her	406	40	M6.5e-9.5e	23	5.0	0.445	γ_1	3
RU	485	43	M6e-9	23	5.7	0.344	γ_1	47
R Hor	408	40	M5e-8eII-III	24	7.0	0.370	α_3	13
R Hya	389	49	M6e-9eS(Tc)	15	5.0	0.434	γ_1	1247
S	257	49	M4e-8e	16	4.9	0.481	β_3	
T	299	49	M3e-9:e	16	4.8	0.458	β_3	1
X	301	42	M7e-8.5e	15	4.4	0.406	α_3	3
RS	339	45	M6e	14	4.1	0.380	β_1:	1
RU	332	35	M6e-8.8e	26	5.6	0.299	α_2	156
S Ind	400	41	M6e-M8eII-Ib	22	6.8	0.231	α_2:	
Y	304	52	M6(II)e-7e	14	—	0.392	—	
R LMi	372	41	M6.5e-9.0e(Tc:)	24	5.5	0.384	α_4	3
T Lep	368	47	M6e-9e	15	4.6	0.282	β_1	4
RR Lib	277	47	M4e-8e	15	5.6	0.450	α_2	1
RS	218	48	M4e-8.5e	15	4.5	0.458	β_2	1
RU	317	46	M5e-6e	17	5.9	0.436	α_4	1
R Lup	236	48	M5e	14	4.0	—	—	
Y	397	37	M7e	24	5.3	0.275	α_2	1
RW	197	36	Mb	15	—	0.284	—	
U Lyn	434	42	M7e-9.5:e	27	4.9	0.371	γ_1	156
V Lyr	374	33	M7e	26	5.1	0.206	α_2	6
RW	504	38	M7e	27	4.3	0.107	α_1	56
U Mic	334	39	M5e-7e	24	5.2	0.274	α_2	56
V Mon	341	46	M5e-8e	16	6.1	0.466	α_4	1
FX	429	35	M1-8	28	—	0.335	—	6
T Nor	241	41	M3e-6e	25	5.8	0.329	α_4	1
R Oct	405	44	M5.5e	15	4.5	0.325	α_2	
S	259	42	M4(II)e-5e	22	5.1	0.380	α_4	
U	308	47	M4e-6(II-III)e	16	5.7	0.411	β_2	1
R Oph	307	45	M4e-6e	16	5.7	0.454	α_4	1
T	367	36	M6.5e	15	4.2	0.367	α_2	
X	329	53	M5e-9e	15	2.0	0.447	β_1	12
RR	292	46	M3e-7	15	5.7	0.456	α_4	1
RT	426	36	M7e(C)	22	5.5	0.339	α_2	156
SS	181	47	M5e	16	4.8	0.462	β_1	1
S Ori	414	48	M6.5e-9.5e	15	4.5	0.374	β_1	124
U	368	38	M6e-9.5e	26	5.7	0.420	α_3	13
BK	354	50	M7e	16	—	0.448	—	1
W Pav	283	40	M4e-7e	24	5.1	0.316	α_4	
P Peg	378	44	M6e-9e	22	5.4	0.398	α_3	13
Z	335	50	M6e-8.5e(Tc)	15	4.8	0.376	β_2	1
RV	397	38	M6e	29	4.7	0.235	α_2	17
SW	396	42:	M4e	16	—	0.371	—	
TU	322	45	M7e-8e	15	—	0.347	—	1

Table 1a (continued)

Star name	Period (day)	$f\times 10^2$	Spectral type	LRS class	$\langle\Delta M_v\rangle$	log S_{12}/S_{25}	l.c.c. (55)	Remarks
PZ Per	396	21	M8	27	—	0.223	—	
S Pic	428	36	M6.5e-8e(II-III)	25	5.7	0.338	α_2	16
R Psc	345	44	M3e-6e	22	6.1	0.343	α_3	1
S	405	42	M5e-7e	23	5.4	0.358	α_2	1
U Pup	318	41	M5e-8e	25	4.3	0.235	α_2	1
Z	509	38	M4e-9e	29	6.4	0.301	α_1	13
RW	341	47	M3e-6e	17	—	0.424	—	1
AS	325	50	M7e-9	15	3.2	0.403	—	1
CH	506	19	Me	23	—	0.285	—	17
R Ret	278	48	M4e-7.5e	15	5.7	0.437	α_4	1
KK Sge	438	40	M7	29	—	0.231	—	
NO	345	50:	M5	15	—	0.402	—	
PT	530	40	M10	26	—	0.333	—	7
PV	435	60	M6	15	—	0.422	—	
R Sgr	270	46	M4e-6e	16	5.2	0.490	β_2	1
Z	450	47	M4e-6(Se)	22	7.4	0.354	α_2	7
RR	336	43	M4e-9e	23	6.4	0.418	α_4	156
RT	306	47	M5e-7e	16	6.3	0.451	α_4	1
RU	240	43	M3e-6e	23	5.6	0.405	α_4	1
RV	316	47	M4e-9	16	6.3	0.451	β_1	1
SW	290	51	M5e-8	15	—	0.410	β_1	1
Z Sco	343	49	M5.5e:-7e	16	4.2	0.422	β_1	1
RU	371	54	M7II-IIIe	16	4.0	0.447	γ_1	1
RW	389	40	M5e	27	—	0.244	α_2	3
S Scl	363	48	M3e-9e (Tc)	15	6.2	0.435	γ_1	15
AA Sct	265	25	M4-6	14	—	0.438	—	7
R Ser	356	41	M5IIIe-9e	22	6.5	0.430	α_4	145
S	372	43	M5e-6e	22	4.8	0.371	γ_1	13
R Tau	321	41	M5e-9e	21	5.6	0.287	γ_1	13
RX	332	47	M6e-7e	15	4.4	0.374	α_4	156
IK	470	50	M6e-10e	26	—	0.290	—	37
R Tel	462	43	M5IIe-7e	15	6.2	0.393	γ_1	
R Tri	267	44	M4IIe-8e	16	5.5	0.464	β_2	15
R UMa	302	39	M3e-9e	23	5.5	0.235	α_3	5
S UMi	321	50	M6e-9e	21	3.6	0.393	β_2	1
W Vel	395	44	M5-8IIIe	22	4.8	0.378	α_3	16
Y	450	40	M8e-9.5	23	4.3	0.314	α_1	1
Z	411	46	M9e	15	5.3	0.405	γ_1	1
RS	410	40	M7e	21	—	0.346	—	1
RW	443	50	M7III (II)e	15	—	0.387	—	1
R Vir	146	50	M3.5IIIe-8.5e	17	4.6	0.452	β_2	14
S	375	45	M6IIIe-9.5e	16	5.7	0.391	α_4	145
RS	354	37	M6III-8e	24	5.8	0.221	α_3	13
S Vol	395	54	M4e	16	5.0	0.422	β_1	1

Remarks to Table 1

1: period varies, 2: visual binary, 3: H_2O, OH, SiO maser/emission, 4: SiO maser, 5: H_2O maser, 6: OH maser/emission, 7: see special note below.

Special notes

Table 1a: SV And – maximum magnitude varies periodically; R Aql – radio bursts; R Cas – sometimes H_2O emission; T Cas – ZrO bands in the IR region; MP Cas – in the nebula NGC 7635 and its log S_{12}/S_{25} too small; Z Cyg – its log S_{12}/S_{25} is too low; RU Her – composite spectrum at minimum (a companion ?); R Hya – not in Stevenson (1984); RV Peg – magnitude at maximum varies by more than 3^m; CH Pup – f value, if correct, is the lowest; PT Sge – p component of a close binary; Z Sgr – not in Stevenson (1984); AA Sct – its period is 153 days and $f=0.43$ according to Kukarkin et al. (1969): this value of f will match better with its value of log S_{12}/S_{25}; IK Tau – the value of log S_{12}/S_{25} is rather low and is more appropriate for $f\leqq 0.43$, unless affected by other conditions.

Table 1b. Data for S spectral type Miras

Star name	NSS no.	Period (days)	$f \times 10^2$	Spectral class	LRS class	$\langle \Delta Mv \rangle$	log S_{12}/S_{25}	l.c.c. (55)	Remarks
W And	49	396	42	S6, 1e-9, 2e	22	6.3	0.366	α_3	
X And	6	346	37	S2, 9e-5, 5e	16	5.8	0.400	α_3	
RW And	14	430	36	S6, 2e	22	6.1	0.290	α_2	
W Aql	1115	490	37	S3, 9e-6, 9e	22	5.7	0.372	α_2	7
T Cam	103	373	47	S4, 7e-8.5, 8e	17	5.8	0.539	γ_1	7
S Cas	28	612	43	S3, 4e-5, 8e	22	5.1	0.243	γ_1	
W Cet	1346	351	50	S6, 3e-9, 2e	16	6.8	0.525	γ_1	7
R Cyg	1150	426	35	S2.5, 9e-6, 9e (Tc)	22	6.4	0.304	α_3	2
R Gem	307	370	36	S2, 9e-8, 9e(Tc)	16	6.4	0.457	α_4	27
R Lyn	283	379	44	S2.5, 5e-6, 8e:	16	5.9	0.502	α_4	
RR Mon	326	395	39	S7, 2e-8, 2e	16	5.6	0.363	α_2	1
ST Sgr	1096	395	44	S4, 3e-9, 5e	21	6.2	0.431	α_1	
RT Sco	954	449	39	S7, 2	22	9.0:	0.380	α_2:	

Table 1b: W Aql – composite spectrum near minimum, a companion (F5-8) may exist; T Cam – spectrum resembles class R(HD catalogue); W Cet – f value from Kukarkin et al. (1969); R Gem – spectrum resembles class R (HD catalogue)

value is indicated by the line bracketing the extreme values at that value of f; partly, this range may be due to difference in phases at which observations were made, besides other variations among individuals stars. We have excluded Z Cyg, MP Cas and IK Tau in averaging as their values are too low compared to other stars of similar f. Hence using mean values at each value of f is preferable to derive any conclusion, rather than individual values. We have preferred to use fluxes observed by IRAS itself rather than taking

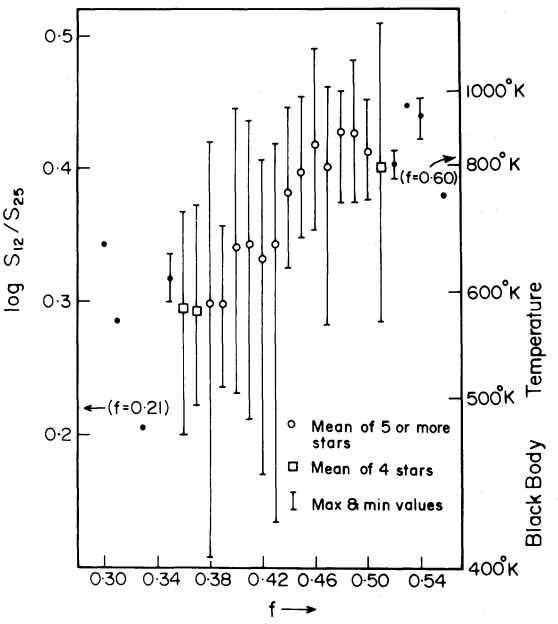

Fig. 3. Plot of flux density ratio, log S_{12}/S_{25}, at 12 and 25 μm from IRAS against f values for M Miras. Circles denote average of 5 or more stars and squares of 4 stars. The vertical lines give the extreme range for a given value of f. Black body temperature is given on the left. Z Cyg, MP Cas and IK Tau have not been included in averaging; see text for the reasons

one of the near-IR wavelengths like 2.2 μm or 3.6 μm for the colour index to ensure that the fluxes going into the colour index determination correspond to the same phase for a given star. The figure shows that log S_{12}/S_{25} has a tendency to increase as f increases; i.e. the emission is from grains at higher temperature for stars with higher value of f. This implies that the circumstellar shell, where the grains are centred, is located farther out from the stellar surface when f is small than when f is large. The problem is complex but can be qualitatively understood if f is inversely correlated to the strength of the outward shock (cf Vardya et al., 1986). A stronger shock drives the grains farther out from the surface than a weaker shock, thus giving rise to cooler grains when f is small than when f is large. Whether this is really so requires detailed caculations of shock propelled circumstellar shell with condensation chemistry.

The mean values of log S_{12}/S_{25} appear to cluster around three values, 0.3, 0.34 and 0.4. If this is not due to selection effect, this may be due to the composition and size distribution of grains for stars with different values of f. It appears that the mean value of log S_{12}/S_{25} reaches a peak at $f=0.48$ and decreases thereafter as f increases. Whether this is statistical or real is difficult to say as the number of stars with $f \geqq 0.51$ are very few.

Note that even the largest value of log S_{12}/S_{25} in Fig. 3 corresponds to a black body colour temperature of about 1000 K, and if the grains have an emissivity proportional to $1/\lambda$, then to grain temperature of 500 K or less; hence grains exist even when silicate emission is absent.

Figure 4 gives a plot of mean values of log S_{12}/S_{25} vs the LRS spectral class. The point at LRS class 29 includes two stars with LRS class 69, as objects of class $m=6$ are qualitatively similar to that of $m=2$ (cf Gal et al., 1987). The circles are mean of 6 or more stars, the pentagon for LRS class 26 for 5 stars and the triangle for 28 is mean of 3 stars only. The figure shows that log S_{12}/S_{25} decreases as the strength of silicate emission band, represented by the second digit (n) of the LRS class, increases, if we join the mean of 6 or more points. Note that the point for LRS = 26 shifts very close to the mean curve if U Ori is neglected; the value log S_{12}/S_{25}

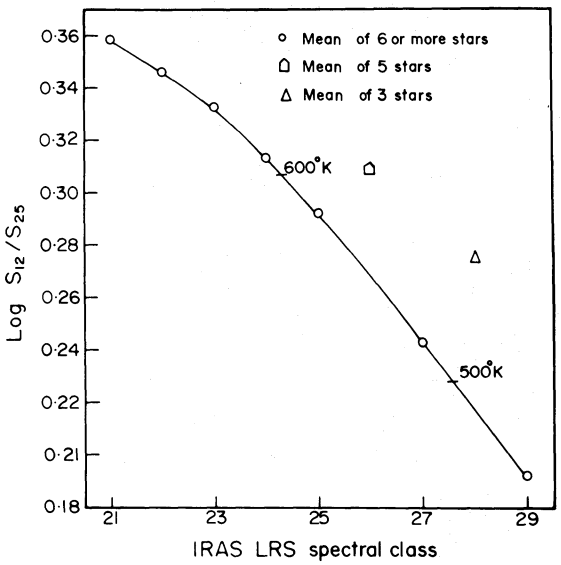

Fig. 4. Plot of mean flux density ratio, log S_{12}/S_{25} vs. LRS spectral class. Circles denote mean of 6 or more stars, pentagon for 5 stars, and triangles of 3 stars. Solid line is a free hand curve of average values of 6 or more stars. The horizontal bars denote black body temperature

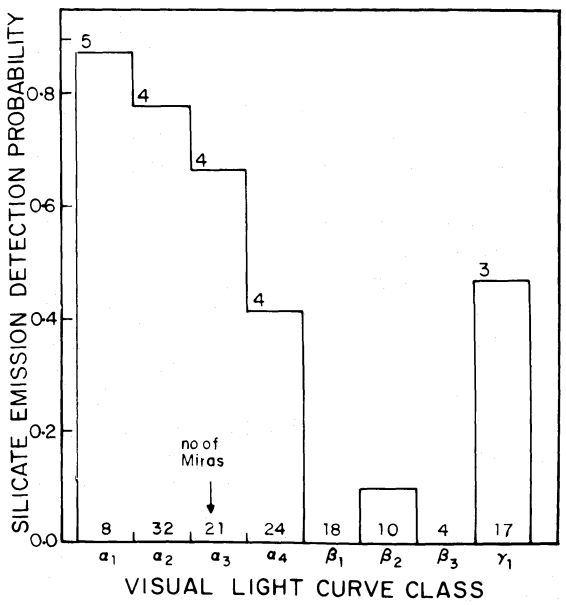

Fig. 5. Detection probability for silicate emission in M Mira variables for different visual light curve classes (Ludendorff). The number of stars in each visual light curve class is given at the bottom. The numbers at the top give mean value of the strength of the silicate emission feature as measured by n of LRS spectral class mn

for this star is very large for this LRS class. This essentially implies that, on the average, the circumstellar dust temperature is lower for stars with stronger 9.7 μm silicate emission. No correlation was found for log S_{60}/S_{25} vs. log S_{12}/S_{25} or LRS class.

If one looks at the light curves, one finds that it is not always easy to determine the f value. Besides, using f value implies that the shape of light curves are similar except for the steepness of the ascending branch. This is of course not true. Though f value has been found to be a useful parameter, it is worth examining the probability of detecting silicate emission based on the shape of the light curve. We will use the Ludendorff's classification, which is partly based on the steepness of the ascending branch of the light curve. In Table 1, visual light curve class (l.c.c. 55), as given by Vardya (1988), is also given. Figure 5 gives the probability of detection of silicate emission in a sample of 131 stars. The highest probability of 88% is for α_1 stars, and decreases to 42% for α_4 class stars. The detectability is essentially zero for β_1, β_2 and β_3 stars but for γ_1 stars it is 47%. There are no stars with β_4 and γ_2 class in our sample. However, the two γ_2 stars in the sample of Vardya (1988), both show silicate emission, with LRS spectral class 22 and 23. Silicate emission feature strength, as measured by the second digit (n) of the LRS spectral class is on the average, highest for the α_1 class ($n=5.4\pm2.9$, 7 stars), decreases (to $n\cong4\pm2.2$) for (α_2, α_3, α_4)-classes, and is lowest for the γ_1 class ($n=3.1\pm1.3$, 8 stars). The fact that the probability of detection and the variation of average strength of silicate emission is similar but different than the detection of 1.35 cm H_2O line in M Miras (Vardya, 1987) is perhaps a reflection of their origin. Silicate emission strongly depends on the steepness of the ascending branch of the light curve.

The mean values of log S_{12}/S_{25} are smaller for M Miras with silicate emission (LRS Spectral class 2n and 6n) than without it for visual light curve classes α_1, α_2, α_3, α_4 and γ_1. The difference can be as large as 0.08. Though the number of stars are small in a few cases, this indicates that the far infrared colour temperatures of the circumstellar shells around M Miras is lower by about $\sim$100–150 K for stars with silicate emission than without it. Further, mean value of log S_{12}/S_{25} is the smallest for α_1 class and increases as we proceed to α_2, α_3, α_4 and γ_1 classes. Thus, the value of log S_{12}/S_{25} anticorrelates with the strength of the silicate emission as well as with the probability of detecting silicate emission.

Table 1b for S Miras follow M stars in the sense that all seven LRS class 2n stars have $f\leqq0.45$ though two stars with $f\leqq0.45$ have LRS class 1n also. All S Miras with LRS class 2n have weak silicate emission as n is either 1 or 2; this is not surprising as elemental abundance ratio oxygen/carbon is very close to unity in the photosphere of these stars and in all probability in the circumstellar shall as well and hence not very conducive to formation of silicates. It is possible that condensates formed in these stars have slightly different composition and structure, and hence have peak slightly away from 9.7 μm, or have a broad shallow feature, resulting in weak features in LRS 2n classification (cf. Little, Little-Marenin and Price 1987). It is, however, surprising that not a single S Mira show strong silicate feature, indicating remnant M phase shell when even a C Mira, RV Cen shows it (Little-Marenin and Wilton 1986). This may imply a gradual change from M to S phase.

4. Discussion and conclusions

We have found here that IRAS LRS spectral class is useful in deriving statistical properties, though it is no substitute for detailed analysis using spectra itself (cf. Onaka and de Jong, 1987). Using it, we have confirmed the findings of Vardya et al. (1986), that only those M Miras show silicate emission which have

$f \leqq 0.45$; however, there are M Miras with $f \leqq 0.45$ which do not show silicate emission. Though strong emission features are present for all values of f, Miras with $f \leqq 0.37$ exhibiting silicate emission correspond to LRS class (2 or 6)4 or stronger only. Alternatively, it is found that M Miras with visual light curve class α_1 has the highest probability of showing silicate emission feature and decreases gradually as we go to α_2, α_3, and α_4 visual light curve classes; average strength of the silicate feature is highest for α_1 class stars and somewhat lower for α_2, α_3, and α_4. This can be understood qualitatively in terms of the explanation given in Vardya et al. (1986) assuming steepness of the ascending branch of the visual light curve being a measure of the shock strength, produced by pulsation, which drives the mass loss in these stars resulting in complete freezing of the condensation close to the surface of the star. The fact that some M Miras with $f \leqq 0.45$ do not show silicate emission may indicate its depencence on other parameters; one of them may be mean visual light amplitude. What these parameters are and how their combination work needs to be investigated. A quantitative treatment of pulsation, shock waves, and condensation chemistry is essential for proper understanding.

S Miras have elemental abundance ratio $O/C > 1$ but very close to unity and are therefore akin to M stars. The fact that S stars follow the same trend as M Miras is therefore understandable.

Acknowledgements. It is a pleasure to thank Prof. K.V.K. Iyengar for providing a copy of IRAS Point Source Catalogue for objects with LRS Spectra. The author is thankful to the referee, Dr. R. Papoular for his useful comments.

References

Beichman, C.A., Neugebauer, G., Habing, H.J., Clegg, P.E., Chester, T.J.: 1985, IRAS Catalogs and Atlases Explanatory Supplement, JPL Publication D-1855

Gal, O., de Muizon, M., Papoular, R., Pegouire, B.: 1987, *Astron. Astrophys.* **183**, 29

Kholopov, P.N.: 1985, *General Catalogue of Variable Stars*, 4th Edition, Nauka Publishing House, Moscow, Vols. 1, 2 and 3

Kukarkin, B.V., Kholopov, P.N., Efremov, Y.N., Kukarkina, N.P., Kurochkin, N.E., Medvedeva, G.I., Perova, N.B., Fedorovich, V.P., Frolov, M.S.: 1969, *General Catalogue of Variable Stars*, 3rd Edition, Nauka Publishing House, Moscow, Vols. 1 and 2 and several supplements

Little, S.J., Little-Marenin, I.R., Price, S.T.: 1987, in *Cool Stars, Stellar Systems, and the Sun*, eds. J.L. Linsky, R.E. Stencel, Springer, Berlin, Heidelberg, New York, p. 377

Little-Marenin, I.R., Wilton, C.: 1986, in *Cool Stars, Stellar Systems, and the Sun*, eds. M. Zeilik, D.M. Gibson, Springer, Berlin, Heidelberg, New York, p. 420

Ludendorff, H.: 1928, in *Handbuch der Astrophysik*, Verlag J. Springer, Berlin, Vol. 6, Chap. 2, p. 49

Onaka, T., de Jong, T.: 1987, in *Late Stages of Stellar Evolution*, eds. S. Kwok, S.R. Pottasch, Reidel, Dordrecht, p. 97

Olnon, F.M., Raimond, E.: 1986, IRAS Catalogues and Atlases. Atlas of Low Resolution Spectra, *Astron. Astrophys. Suppl.* **65**, 607

Stephenson, C.B.: 1984, *A General Catalogue of Galactic S Stars*, 2nd edition, Publ. Warner and Swasey Observatory, Vol. 3, No. 1

Vardya, M.S., de Jong, T., Willems, F.J.: 1986, *Astrophys. J. Letters.* **304**, L29

Vardya, M.S.: 1987, *Astron. Astrophys.* **182**, 75

Vardya, M.S.: 1988, *Astron. Astrophys. Suppl.* **73**, 181